



This is the accepted manuscript made available via CHORUS. The article has been published as:

## Quantum-Enhanced Metrology for Molecular Symmetry Violation Using Decoherence-Free Subspaces

Chi Zhang, Phelan Yu, Arian Jadbabaie, and Nicholas R. Hutzler

Phys. Rev. Lett. **131**, 193602 — Published 8 November 2023

DOI: [10.1103/PhysRevLett.131.193602](https://doi.org/10.1103/PhysRevLett.131.193602)

# Quantum-Enhanced Metrology for Molecular Symmetry Violation using Decoherence-Free Subspaces

Chi Zhang,<sup>1,\*</sup> Phelan Yu,<sup>1</sup> Arian Jadbabaie,<sup>1</sup> and Nicholas R. Hutzler<sup>1</sup>

<sup>1</sup>*California Institute of Technology, Division of Physics, Mathematics, and Astronomy, Pasadena, CA 91125*

(Dated: October 13, 2023)

We propose a method to measure time-reversal symmetry violation in molecules that overcomes the standard quantum limit while leveraging decoherence-free subspaces to mitigate sensitivity to classical noise. The protocol does not require an external electric field, and the entangled states have no first-order sensitivity to static electromagnetic fields as they involve superpositions with zero average lab-frame projection of spins and dipoles. This protocol can be applied with trapped neutral or ionic species, and can be implemented using methods which have been demonstrated experimentally.

Precision measurements of time-reversal (T) symmetry violation in molecular systems provide stringent tests of new physics beyond the Standard Model [1]. For example, searches for the electron's electric dipole moment (eEDM) have excluded a broad parameter space of T violating leptonic physics at energy scales up to  $\sim 50$  TeV [2–5]. Experiments aiming to laser cool and trap eEDM-sensitive neutral molecules [6–11] are currently under construction and promise significantly improved measurement precision. The immediate impact of cooling and trapping is the substantially longer coherence time compared to beam experiments, a result of both long trapping time and easier field control for quasi-stationary molecules confined in a small volume. Furthermore, quantum metrology techniques [12, 13], such as entanglement and squeezing, promise routes to additional enhancement of eEDM sensitivity. However, a specific scheme providing metrological gain without added susceptibility to classical noise from electromagnetic fields has, to our knowledge, not yet been conceived.

Additionally, contemporary eEDM searches with molecular ions are conducted in non-stationary rotating traps [2, 14], since an external electric field is used to polarize the molecules. Although various improvements will be implemented for near-future experiments [15, 16], molecule motion in the rotating trap during spin precession remains a challenge for implementing entanglement-enhanced metrology.

In this manuscript, we show that the eEDM can be observed as a coupling between two or more entangled molecules within a decoherence-free subspace. The eEDM sensitivity scales linearly with the entangled molecule number, thereby offering Heisenberg-limited sensitivity beyond the standard quantum limit, while the susceptibility to electromagnetic fields remains mitigated. In addition, the molecules do not have to be aligned in the lab frame by an external electric field; instead, they are prepared in orthogonal superpositions of opposite parity states. As a result, the scheme is applicable to neutral molecules in optical lattices or tweezer ar-

rays [17, 18] as well as molecular ions in quasi-stationary traps [19, 20], which enable entanglement generation and are a well-established platform for precision measurement [21, 22]. Importantly, the entangled molecular states involved are experimentally achievable using existing entanglement protocols [23–29], some of which have been demonstrated recently [17–19], together with single molecule operations [30, 31]. Furthermore, the protocol is readily compatible with a broad range of molecules. Our discussion here focuses on the eEDM as an example, but the method can be straightforwardly extended to measure other T violating moments, including the nuclear Schiff moment [32] and nuclear magnetic quadrupole moment [33].

The energy shift of the eEDM ( $d_e$ ) in an effective internal molecular electric field ( $\mathcal{E}_{\text{eff}}$ ) is  $d_e \cdot \mathcal{E}_{\text{eff}}$ . The internal field points along the molecule axis ( $\hat{n}$ ) and its amplitude is determined by the electronic structure of the molecule, while the eEDM is collinear with the total electron spin ( $S$ ). Conventional eEDM experiments [1–3, 34, 35] orient the molecule axis in the lab frame by mixing opposite parity states with an external electric field, and subsequently polarize the electron spin in the lab frame as well. The eEDM interaction then manifests as a small spin-dependent energy shift, measured by performing spin precession in the polarized molecules. However, the polarized molecular dipoles and electron spins also make these experiments sensitive to uncontrolled external fields. As a consequence, the most common quantum metrology methods, such as spin squeezing [36–38], increase sensitivity to external electromagnetic fields by the same amount as the gain in eEDM sensitivity. The resulting increased susceptibility to decoherence and systematic errors from these fields, which are a main concern for eEDM experiments, can counteract the eEDM sensitivity boost.

Here we instead probe the eEDM as a *coupling* between two opposite-parity states in a molecule. We first consider the effects of this coupling in a single molecule to build understanding of the system, and then discuss

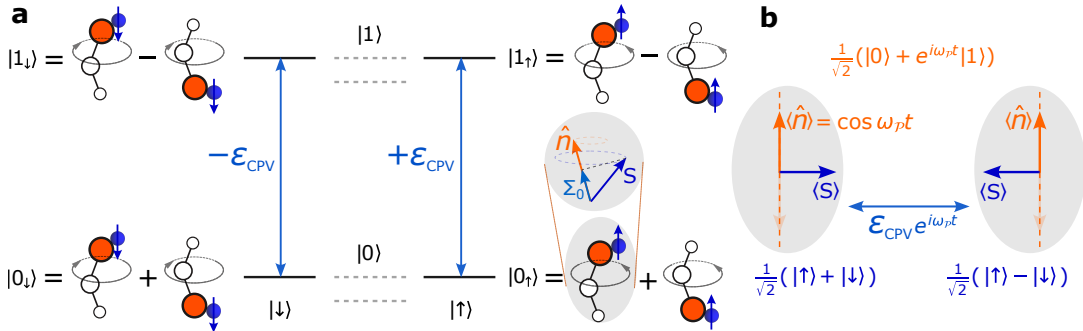


FIG. 1. (a) A typical level diagram of a parity-doubled molecule, for example a triatomic bending mode [9]. Molecule eigenstates  $|0\rangle$  and  $|1\rangle$  are superpositions of molecular dipole orientation. They have magnetic sublevels, the stretched states (thick levels)  $|\uparrow\rangle$  and  $|\downarrow\rangle$  represent electron spin up and down in the lab frame. The dashed levels in the middle indicate magnetic sublevels resulting from electron spin coupling with other angular momenta, which are not needed in our scheme. The insets show the spin  $S$  (dark blue arrow) projection  $\Sigma$  on the molecule axis  $\hat{n}$  (light blue arrow) in the molecule frame. The eEDM gives a coupling  $\pm\epsilon_{CPV}$  between  $|0\rangle \leftrightarrow |1\rangle$ , and the sign of the coupling depends on the spin. (b) The effective electric field along the molecule axis couples spin states. In the lab frame, due to the energy difference  $\omega_P$  between  $|0\rangle$  and  $|1\rangle$ , the orientation of the molecule axis is oscillating, thus the coupling, the spin-precession direction, is also oscillating.

how we can engineer entangled states in a two (or more) molecule system which have Heisenberg-limited sensitivity ( $\propto N$ ) to the eEDM but without concurrent increases in collective electric or magnetic field sensitivity.

In Fig. 1, we provide an example of a single molecule in the parity-doubled bending mode of a  ${}^2\Sigma$  triatomic molecule [9], though the method should be generalizable to other types of parity-doubled states. The opposite-parity states are labeled as  $|0\rangle$  and  $|1\rangle$ , and the spin states in the lab basis are labeled by  $|\uparrow\rangle$  and  $|\downarrow\rangle$ . The eEDM causes a spin-dependent coupling between  $|0\rangle \leftrightarrow |1\rangle$  with a coupling strength  $\epsilon_{CPV} = \langle 0_\uparrow | \mathcal{E}_{\text{eff}} d_e \Sigma | 1_\uparrow \rangle = 2\mathcal{E}_{\text{eff}} d_e \Sigma_0$ , where  $\Sigma = S \cdot \hat{n}$  is the projection of spin on the molecule axis and  $\Sigma_0$  is the expectation value of  $\Sigma$  when averaged over other angular momentum quantum numbers of the molecule wavefunction [39]. The coupling changes sign to  $-\epsilon_{CPV}$  for the time-reversed state  $|\downarrow\rangle$ .

In a superposition state such as  $\frac{1}{2}(|0\rangle + |1\rangle)(|\uparrow\rangle + e^{i\theta} |\downarrow\rangle)$ , which corresponds to an orientation of  $\mathcal{E}_{\text{eff}}$  perpendicular to the electron spin, the eEDM interaction causes spin precession that changes the phase  $\theta$  of the spin superposition. Note that this is conceptually similar to the usual idea of creating a superposition of  $|0\rangle, |1\rangle$  by polarizing the molecule with a static external electric field. However, here we consider creating a superposition of these states without static applied fields, meaning that the orientation of the molecular dipole, and therefore  $\mathcal{E}_{\text{eff}}$ , will be oscillating in the lab frame at a frequency given by the parity splitting  $\omega_P$  (typically  $\sim 2\pi \times 100$  kHz to  $\sim 2\pi \times 100$  MHz) between  $|0\rangle$  and  $|1\rangle$  [9]. Thus, the eEDM spin precession ( $\lesssim 100$   $\mu$ Hz) can only accumulate phase in the frame rotating at  $\omega_P$ ; in the lab frame, the direction of spin precession oscillates rapidly and averages to zero, so there is no eEDM-induced energy shift or spin precession.

However, with *two* (or more) molecules, we can engineer states where eEDM precession does not average to zero, yet the oscillation in the lab frame makes the molecules highly insensitive to external fields. Furthermore, we shall see that these states have a metrological gain in sensitivity due to entanglement. We first discuss the case for  $N = 2$  molecules to build understanding of the protocol, and later discuss extension to larger systems. We denote the superpositions  $\frac{1}{\sqrt{2}}(|0\rangle + e^{i\omega_P t} |1\rangle) = |\widetilde{\uparrow}\rangle$  and  $\frac{1}{\sqrt{2}}(|0\rangle - e^{i\omega_P t} |1\rangle) = |\widetilde{\downarrow}\rangle$ , suggestive of the fact that these states have opposite orientation of the (rotating) molecular dipole. Consider two molecules in the state  $|\widetilde{\uparrow}\widetilde{\downarrow}\rangle$ , as shown in Fig. 2, where we label rotating frame spin states using  $|\widetilde{\uparrow}\rangle$  and  $|\widetilde{\downarrow}\rangle$ . The rotation of the frame is described as  $H_{\text{rot}} = \hbar\omega_P \tilde{\sigma}_x$  in the rotating frame basis [40] (also see Supplemental Material [41]). An eEDM shifts  $|\widetilde{\uparrow}\rangle$  and  $|\widetilde{\downarrow}\rangle$  oppositely, as they have opposite relative orientations of electron spins and molecular dipoles. Therefore, an eEDM couples the degenerate singlet and triplet pair states with zero total spin projections. These states constitute a decoherence-free subspace as the molecular electric and magnetic dipole moments have zero average projection on the laboratory fields and are therefore insensitive to them to first order. This is conceptually similar to the eEDM coupling in a hyperfine clock transition [42].

Similar to the single molecule case, the eEDM has little effect on the eigenstates of  $H_{\text{rot}}$ . However, now we can switch on and off the eEDM spin precession by applying a radio-frequency (rf) magnetic field  $B$  in phase with the rotating frame (this is challenging for a single molecule; see Supplemental Material). The rf magnetic field is described by  $H_B = \Omega_B \tilde{\sigma}_z$ , with  $\Omega_B$  the interaction strength ( $\Omega_B \approx \mu_B B$  for  ${}^2\Sigma_{1/2}$  electronic states), and it

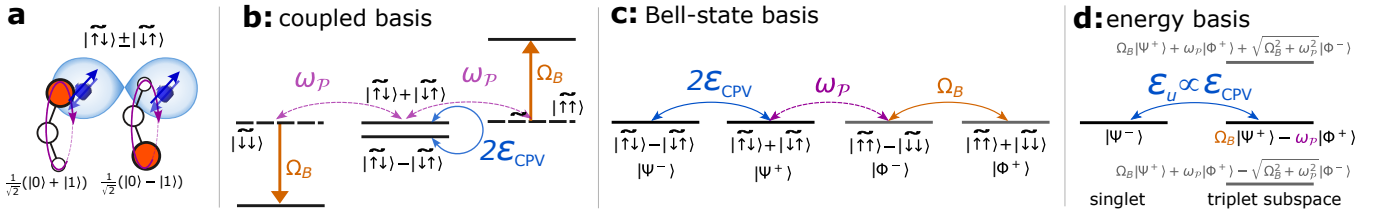


FIG. 2. (a) eEDM interaction for two molecules in opposite molecular dipole superposition states  $|\tilde{\uparrow}\uparrow\rangle$  and  $|\tilde{\downarrow}\downarrow\rangle$  and entangled spin state  $|\tilde{\uparrow}\downarrow\rangle \pm |\tilde{\downarrow}\uparrow\rangle$ . (b) In the rotating frame, an eEDM couples the degenerate singlet and triplet pair states with zero spin projections. The triplet states are coupled by rotation of the frame. A magnetic field shifts  $|\tilde{\uparrow}\uparrow\rangle$  and  $|\tilde{\downarrow}\downarrow\rangle$  oppositely and suppresses the coupling of the rotation. This is equivalent to (c) in the Bell-state basis, where  $|\Psi^\pm\rangle = \frac{1}{\sqrt{2}}(|\tilde{\uparrow}\downarrow\rangle \pm |\tilde{\downarrow}\uparrow\rangle)$  and  $|\Phi^\pm\rangle = \frac{1}{\sqrt{2}}(|\tilde{\uparrow}\uparrow\rangle \pm |\tilde{\downarrow}\downarrow\rangle)$ . The eEDM interaction couples  $|\Psi^-\rangle \leftrightarrow |\Psi^+\rangle$ , which is separated from other couplings by an external magnetic field. The rotation couples  $|\Psi^+\rangle \leftrightarrow |\Phi^-\rangle$ , and an rf magnetic field in phase with the molecule rotation couples  $|\Phi^-\rangle \leftrightarrow |\Phi^+\rangle$ . As a result, in (d), the eEDM interaction effectively couples  $|\Psi^-\rangle$  to the unshifted state of the three-level system ( $|\Psi^+\rangle \leftrightarrow |\Phi^-\rangle \leftrightarrow |\Phi^+\rangle$ ) with a reduced coupling strength of  $4\varepsilon_{CPV} \frac{\Omega_B}{\sqrt{\Omega_B^2 + \omega_p^2}}$ , which reaches 90% of the maximum  $4\varepsilon_{CPV}$  for  $\Omega_B \gtrsim 2\omega_p$  and 98% of the maximum for  $\Omega_B \gtrsim 5\omega_p$ .

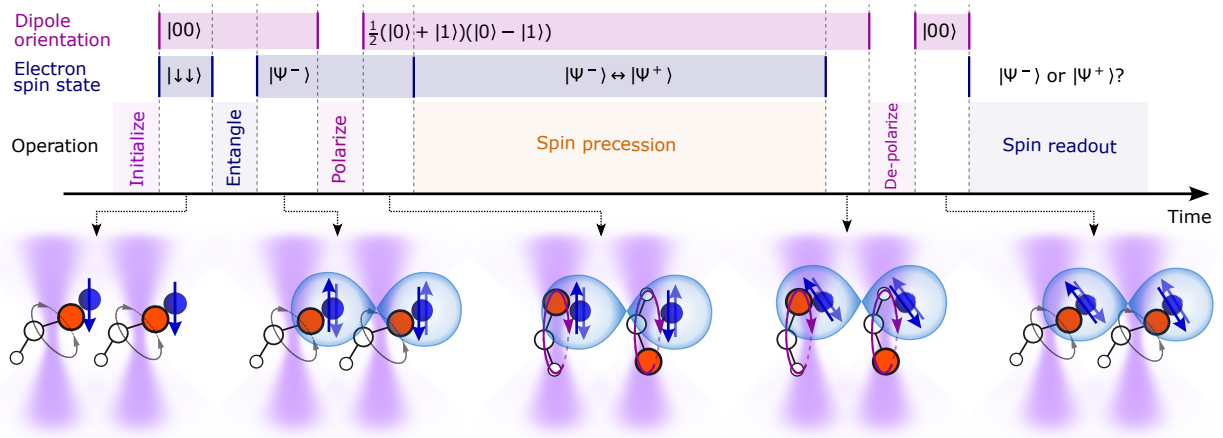


FIG. 3. Experimental sequence for the eEDM measurement. The steps are indicated by the boxes on the time line. The purple boxes represent operations on molecule orientation, and the blue boxes mostly act on the spin degree of freedom. The spin precession enabled by an rf magnetic field is represented by the orange box. The molecule orientation and spin state are specified above the sequence boxes, and shown schematically in the illustrations below it. See more details in text.

shifts  $|\tilde{\uparrow}\uparrow\rangle$  and  $|\tilde{\downarrow}\downarrow\rangle$  oppositely, as they have different orientations relative to the rf field. The couplings of  $H_{\text{rot}}$ ,  $H_B$ , and eEDM are shown in Fig. 2(c) in the Bell state basis ( $|\Psi^\pm\rangle = \frac{1}{\sqrt{2}}(|\tilde{\uparrow}\downarrow\rangle \pm |\tilde{\downarrow}\uparrow\rangle)$ ,  $|\Phi^\pm\rangle = \frac{1}{\sqrt{2}}(|\tilde{\uparrow}\uparrow\rangle \pm |\tilde{\downarrow}\downarrow\rangle)$ ).

$H_{\text{rot}}$  and  $H_B$  couple  $|\Psi^+\rangle \leftrightarrow |\Phi^-\rangle$  and  $|\Phi^-\rangle \leftrightarrow |\Phi^+\rangle$ , respectively. The resulting eigenstates are shown in Fig. 2(d); the middle state, whose eigenenergy is not shifted, is  $|u\rangle = \sin\theta|\Psi^+\rangle - \cos\theta|\Phi^+\rangle$ , with the mixing angle  $\theta$  given by  $\tan\theta = \Omega_B/\omega_p$ . Note that these interactions do not couple to  $|\Psi^-\rangle$ . However, the eEDM interaction couples  $|\Psi^-\rangle \leftrightarrow |\Psi^+\rangle$  but with coupling strength much smaller than  $H_B$  or  $H_{\text{rot}}$ . The eEDM therefore induces a resonant coupling  $|\Psi^-\rangle \leftrightarrow |u\rangle$  with a reduced coupling strength of  $\varepsilon_u = 4\varepsilon_{CPV} \frac{\Omega_B}{\sqrt{\Omega_B^2 + \omega_p^2}}$ , which reaches  $\sim 90\%$  of the maximum ( $4\varepsilon_{CPV}$ ) when  $\Omega_B \gtrsim 2\omega_p$ . Note that this is twice the coupling of a fully polarized single

molecule, thereby beating the standard quantum limit. A static magnetic field, or more generally, a magnetic field at a different frequency, causes the phase on the  $|\Psi^+\rangle$  part of  $|u\rangle$  to oscillate and thus the eEDM coupling averages to zero. Consequently, the eEDM spin precession is turned on only when the magnetic field is in-phase. The eEDM spin-precession subspace is also known as a decoherence-free subspace [43]; it is robust to noise since the total spin and dipole projections, and therefore the expectation of electric and magnetic dipole moments, is zero.

The experimental sequence for two molecules, as an example, is illustrated in Fig. 3. Molecules are initialized in  $|0_1 0_\downarrow\rangle$  by optical pumping. Then the spins are entangled in  $|\Psi^-\rangle_{\text{lab}}$  (details about entanglement generation for two and more molecules, as well as an example for two molecules, are in the Supplemental Material). Sub-

sequently, the molecule orientation is prepared in  $|\overline{\uparrow\downarrow}\rangle$ . This can be done in two sub-steps: first drive a global  $\pi/2$ -pulse between  $|0\rangle \leftrightarrow |1\rangle$ , and then apply an AC-Stark shift using a far-detuned laser focused on one of the molecules and imprint a  $\pi$  phase on  $|1\rangle$ . By addressing different molecules, or by changing the detuning of the laser, the direction of eEDM spin precession can be controlled, thus providing “switches” to observe the eEDM [44]. Note that for multiple pairs of molecules trapped simultaneously, this could be performed in parallel across different pairs to mitigate imperfections in the laser pulses. The initial spin state  $|\Psi^-\rangle_{\text{lab}}$  is invariant under rotations and thus is equal to  $|\Psi^-\rangle$  in the rotating frame. Next, when the rf magnetic field is turned on, eEDM spin precession  $|\Psi^-\rangle \leftrightarrow |u\rangle$  starts in the rotating frame. After eEDM spin precession, the magnetic field is turned off and then the orientation of the molecules is rotated back to  $|00\rangle$ . In the lab frame,  $|u\rangle$  is an rf-dressed state, which is oscillating in the triplet subspace of  $\{|\Psi^+\rangle_{\text{lab}}, |\Phi^-\rangle_{\text{lab}}, |\Phi^+\rangle_{\text{lab}}\}$ . After turning off the magnetic field, the population in  $|u\rangle$  is distributed in the triplet subspace but mostly mapped to  $|\Psi^+\rangle_{\text{lab}}$ . Finally, the eEDM spin precession phase, i.e. the phase between  $|\uparrow\downarrow\rangle$  and  $|\downarrow\uparrow\rangle$  components, is measured by a projection measurement in the  $\frac{1}{\sqrt{2}}(|\uparrow\downarrow\rangle \pm i|\downarrow\uparrow\rangle)$  basis by the parity oscillation measurement [17, 18, 45] as described further in the Supplemental Material.

Our scheme has many advantages. The spin precession rate in the entangled basis is two times faster than in a fully polarized single molecule, and it scales linearly with molecule number for the anti-ferromagnetic spin states (i.e. between  $\frac{1}{\sqrt{2}}(|\uparrow\downarrow\uparrow\dots\uparrow\downarrow\rangle + |\downarrow\uparrow\downarrow\dots\downarrow\uparrow\rangle) \leftrightarrow \frac{1}{\sqrt{2}}(|\uparrow\downarrow\uparrow\dots\uparrow\downarrow\rangle - |\downarrow\uparrow\downarrow\dots\downarrow\uparrow\rangle)$  for molecule orientation  $|\overline{\uparrow\downarrow\uparrow\dots\uparrow\downarrow}\rangle$ ), thus realizing a metrological gain from entanglement. More importantly, the eEDM spin precession subspace is decoupled from various environmental noise sources, including magnetic fields, vector and tensor light shifts, etc., since the total spin and dipole projections are zero and the spin precession takes place in a rotating frame where slow noise is averaged out. This is unlike conventional eEDM protocols using polarized molecules in the lab frame, where the eEDM-enhanced entangled states, such as squeezed states or the GHZ state  $\frac{1}{\sqrt{2}}(|\uparrow\uparrow\dots\uparrow\rangle + |\downarrow\downarrow\dots\downarrow\rangle)$ , normally require spins aligned collectively in the lab frame and thus are also increasingly sensitive to magnetic field noise, AC Stark shifts, etc.

Various experimental imperfections, such as infidelity of entanglement generation, imperfect control of laser parameters, stray electric fields, blackbody radiation, and more, are discussed in the Supplemental Material. We estimate that  $\sim 10$  s coherence time is achievable with realistic experimental parameters. Furthermore, the imperfections are independent from the eEDM switch (AC Stark shift from the addressing beam) and thus do not

lead to systematic effects directly, but instead to contrast reduction and increased statistical noise. In particular, the eEDM spin precession is opposite in  $|\overline{\uparrow\downarrow\uparrow\dots\downarrow}\rangle$  versus  $|\overline{\downarrow\uparrow\downarrow\dots\uparrow}\rangle$ , and the spin does not precess in  $|\overline{\uparrow\uparrow\uparrow\dots\uparrow}\rangle$  or  $|\overline{\downarrow\downarrow\downarrow\dots\downarrow}\rangle$ . Other couplings, such as magnetic field gradients oscillating at the parity doubling frequency, are insensitive to the  $\pm$  phase between  $|0\rangle$  and  $|1\rangle$ .

In summary, we have presented a quantum metrology scheme to probe T-violating effects in molecular systems. The Heisenberg scaling is particularly important for the future experiments where the molecules are well-controlled but do not necessarily have large molecule numbers, such as molecules in tweezer arrays and ion traps, as well as rare radioactive molecules [46]. The T-violating interaction causes spin precession in an entangled, decoherence-free subspace in a rotating frame, where the slow noise in the lab frame is averaged out, and the molecules do not need to be polarized by an external electric field. As a result, the scheme is compatible with stationary ion traps, such as the linear Paul trap, in which a powerful toolbox of precision spectroscopy and quantum metrology has been developed, including sympathetic cooling [47], quantum logic spectroscopy [16, 48], ion shuttling [49], micromotion compensation [50], entanglement generation, etc. Furthermore, the direction of spin precession is controlled by the phase of the applied magnetic rf field and the phase of the oscillation of the molecule orientation. In T-violation measurements, systematic effects normally arise from imperfections correlated with the switch of the sign of the T-violating interaction, such as parity state or external electric field. Our eEDM switch is an AC-Stark shift by the far-detuned addressing beam on one of the molecules, which has little correlation with other imperfections, and can be performed in parallel across multiple pairs of molecules. In addition, because of the magnetic field insensitivity, this scheme will also improve the coherence in a shot-noise limited measurement using magnetic molecules, including all laser coolable neutral molecules and certain T-sensitive molecular ions whose ground states are magnetic. These advantages will significantly improve the precision of T-violating new physics searches in the near future.

We acknowledge helpful discussions with Andreas Elben, Manuel Endres, Ran Finkelstein, Andrew Jayich, Dietrich Leibfried, Christopher Pattison, John Preskill, Tim Steimle, Yuiki Takahashi, Michael Tarbutt, Fabian Wolf, Xing Wu and the PolyEDM Collaboration. This work was supported by Gordon and Betty Moore Foundation Award GBMF7947, Alfred P. Sloan Foundation Award G-2019-12502, and NSF CAREER Award PHY-1847550. C.Z. acknowledges support from the David and Ellen Lee Postdoctoral Fellowship at Caltech. P.Y. acknowledges support from the Eddleman Graduate Fellowship through the Institute for Quantum Information and Matter (IQIM).

- 
- \* chizhang@caltech.edu
- [1] M. S. Safronova, D. Budker, D. DeMille, D. F. J. Kimball, A. Derevianko, and C. W. Clark, Rev. Mod. Phys. **90**, 025008 (2018).
- [2] T. S. Roussy, L. Caldwell, T. Wright, W. B. Cairncross, Y. Shagam, K. B. Ng, N. Schlossberger, S. Y. Park, A. Wang, J. Ye, and E. A. Cornell, An improved bound on the electron's electric dipole moment (2023).
- [3] V. Andreev, D. G. Ang, D. DeMille, J. M. Doyle, G. Gabrielse, J. Haefner, N. R. Hutzler, Z. Lasner, C. Meisenhelder, B. R. O'Leary, C. D. Panda, A. D. West, E. P. West, and X. Wu, Nature **562**, 355 (2018).
- [4] C. Cesarotti, Q. Lu, Y. Nakai, A. Parikh, and M. Reece, Journal of High Energy Physics **2019**, 59 (2019).
- [5] R. Alarcon et al., Electric dipole moments and the search for new physics (2022), arXiv:2203.08103.
- [6] X. Alauze, J. Lim, M. A. Trigatzis, S. Swarbrick, F. J. Collings, N. J. Fitch, B. E. Sauer, and M. R. Tarbutt, Quantum Sci. Technol. **6**, 044005 (2021).
- [7] N. J. Fitch, J. Lim, E. A. Hinds, B. E. Sauer, and M. R. Tarbutt, Quantum Sci. Technol. **6**, 014006 (2021).
- [8] B. L. Augenbraun, Z. D. Lasner, A. Frenett, H. Sawaoka, C. Miller, T. C. Steimle, and J. M. Doyle, New J. Phys. **22**, 022003 (2020).
- [9] I. Kozyryev and N. R. Hutzler, Phys. Rev. Lett. **119**, 133002 (2017).
- [10] T. A. Isaev, S. Hoekstra, and R. Berger, Phys. Rev. A **82**, 052521 (2010).
- [11] Z. Lasner, A. Lunstad, C. Zhang, L. Cheng, and J. M. Doyle, Physical Review A **106**, L020801 (2022).
- [12] L. Pezzé, A. Smerzi, M. K. Oberthaler, R. Schmied, and P. Treutlein, Rev. Mod. Phys. **90**, 035005 (2018).
- [13] L. Pezzé and A. Smerzi, Phys. Rev. Lett. **102**, 100401 (2009).
- [14] W. B. Cairncross, D. N. Gresh, M. Grau, K. C. Cossel, T. S. Roussy, Y. Ni, Y. Zhou, J. Ye, and E. A. Cornell, Phys. Rev. Lett. **119**, 153001 (2017).
- [15] K. B. Ng, Y. Zhou, L. Cheng, N. Schlossberger, S. Y. Park, T. S. Roussy, L. Caldwell, Y. Shagam, A. J. Vigil, E. A. Cornell, and J. Ye, Phys. Rev. A **105**, 022823 (2022).
- [16] T. N. Taylor, J. O. Island, and Y. Zhou, Quantum logic control and precision measurements of molecular ions in a ring trap – a new approach for testing fundamental symmetries (2022), arXiv:2210.11613 [physics.atom-ph].
- [17] C. M. Holland, Y. Lu, and L. W. Cheuk, On-demand entanglement of molecules in a reconfigurable optical tweezer array (2022), arXiv:2210.06309.
- [18] Y. Bao, S. S. Yu, L. Anderegg, E. Chae, W. Ketterle, K.-K. Ni, and J. M. Doyle, Dipolar spin-exchange and entanglement between molecules in an optical tweezer array (2022), arXiv:2211.09780.
- [19] Y. Lin, D. R. Leibrandt, D. Leibfried, and C.-w. Chou, Nature **581**, 273 (2020).
- [20] M. Fan, C. A. Holliman, X. Shi, H. Zhang, M. W. Straus, X. Li, S. W. Buechele, and A. M. Jayich, Phys. Rev. Lett. **126**, 023002 (2021).
- [21] S. M. Brewer, J.-S. Chen, A. M. Hankin, E. R. Clements, C. W. Chou, D. J. Wineland, D. B. Hume, and D. R. Leibrandt, Phys. Rev. Lett. **123**, 033201 (2019).
- [22] C. Sanner, N. Huntemann, R. Lange, C. Tamm, E. Peik, M. S. Safronova, and S. G. Porsev, Nature **567**, 204 (2019).
- [23] M. Hughes, M. D. Frye, R. Sawant, G. Bhole, J. A. Jones, S. L. Cornish, M. R. Tarbutt, J. M. Hutson, D. Jakusch, and J. Mur-Petit, Phys. Rev. A **101**, 062308 (2020).
- [24] E. R. Hudson and W. C. Campbell, Phys. Rev. A **98**, 040302(R) (2018).
- [25] K.-K. Ni, T. Rosenband, and D. D. Grimes, Chem. Sci. **9**, 6830 (2018).
- [26] S. F. Yelin, K. Kirby, and R. Côté, Phys. Rev. A **74**, 050301(R) (2006).
- [27] C. Zhang and M. Tarbutt, PRX Quantum **3**, 030340 (2022).
- [28] K. Wang, C. P. Williams, L. R. Picard, N. Y. Yao, and K.-K. Ni, PRX Quantum **3**, 030339 (2022).
- [29] A. Omran, H. Levine, A. Keesling, G. Semeghini, T. T. Wang, S. Ebadi, H. Bernien, A. S. Zibrov, H. Pichler, S. Choi, J. Cui, M. Rossignolo, P. Rembold, S. Montangero, T. Calarco, M. Endres, M. Greiner, V. Vuletić, and M. D. Lukin, Science **365**, 570 (2019).
- [30] J. W. Park, Z. Z. Yan, H. Loh, S. A. Will, and M. W. Zwierlein, Science **357**, 372 (2017).
- [31] P. D. Gregory, J. A. Blackmore, S. L. Bromley, J. M. Hutson, and S. L. Cornish, Nature Physics **17**, 1149 (2021).
- [32] B. Graner, Y. Chen, E. G. Lindahl, and B. R. Heckel, Phys. Rev. Lett. **116**, 161601 (2016).
- [33] V. V. Flambaum, D. DeMille, and M. G. Kozlov, Phys. Rev. Lett. **113**, 103003 (2014).
- [34] J. J. Hudson, D. M. Kara, I. J. Smallman, B. E. Sauer, M. R. Tarbutt, and E. A. Hinds, Nature **473**, 493 (2011).
- [35] J. Baron, W. C. Campbell, D. DeMille, J. M. Doyle, G. Gabrielse, Y. V. Gurevich, P. W. Hess, N. R. Hutzler, E. Kirilov, I. Kozyryev, B. R. O'Leary, C. D. Panda, M. F. Parsons, E. S. Petrik, B. Spaun, A. C. Vutha, and A. D. West, Science **343**, 269 (2014).
- [36] D. J. Wineland, J. J. Bollinger, W. M. Itano, F. L. Moore, and D. J. Heinzen, Phys. Rev. A **46**, R6797 (1992).
- [37] D. J. Wineland, J. J. Bollinger, W. M. Itano, and D. J. Heinzen, Phys. Rev. A **50**, 67 (1994).
- [38] M. A. Perlin, C. Qu, and A. M. Rey, Phys. Rev. Lett. **125**, 223401 (2020).
- [39] A. Petrov and A. Zakhарова, Phys. Rev. A **105**, L050801 (2022).
- [40] H. Loh, K. C. Cossel, M. C. Grau, K.-K. Ni, E. R. Meyer, J. L. Bohn, J. Ye, and E. A. Cornell, Science **342**, 1220 (2013).
- [41] See Supplemental Material [url] for the eEDM coupling in one molecule, an example of experimental sequence, effects of imperfections, scaling to more molecules and choice of molecule species, which includes Refs. [2, 3, 9, 17–19, 29, 39, 42, 44, 45, 51–79].
- [42] M. Verma, A. M. Jayich, and A. C. Vutha, Phys. Rev. Lett. **125**, 153201 (2020).
- [43] T. Monz, K. Kim, A. S. Villar, P. Schindler, M. Chwalla, M. Riebe, C. F. Roos, H. Häffner, W. Hänsel, M. Henrich, and R. Blatt, Phys. Rev. Lett. **103**, 200503 (2009).
- [44] J. Baron, W. C. Campbell, D. DeMille, J. M. Doyle, G. Gabrielse, Y. V. Gurevich, P. W. Hess, N. R. Hutzler, E. Kirilov, I. Kozyryev, B. R. O'Leary, C. D. Panda, M. F. Parsons, B. Spaun, A. C. Vutha, A. D. West, and E. P. West, New J. Phys. **19**, 073029 (2017).
- [45] D. Leibfried, E. Knill, S. Seidelin, J. Britton, R. B. Blakestad, J. Chiaverini, D. B. Hume, W. M. Itano, J. D. Jost, C. Langer, R. Ozeri, R. Reichle, and D. J.

- Wineland, Nature **438**, 639 (2005).
- [46] G. Arrowsmith-Kron, M. Athanasakis-Kaklamanakis, M. Au, J. Ballof, R. Berger, A. Borschovsky, A. A. Breier, F. Buchinger, D. Budker, L. Caldwell, C. Charles, N. Dattani, R. P. de Groote, D. DeMille, T. Dickel, J. Dobaczewski, C. E. Düllmann, E. Eliav, J. Engel, M. Fan, V. Flambaum, K. T. Flanagan, A. Gaiser, R. G. Ruiz, K. Gaul, T. F. Giesen, J. Ginges, A. Gottberg, G. Gwinner, R. Heinke, S. Hoekstra, J. D. Holt, N. R. Hutzler, A. Jayich, J. Karthein, K. G. Leach, K. Madison, S. Malbrunot-Ettenauer, T. Miyagi, I. D. Moore, S. Moroch, P. Navrátil, W. Nazarewicz, G. Neyens, E. Norrgard, N. Nusgart, L. F. Paštka, A. N. Petrov, W. Plass, R. A. Ready, M. P. Reiter, M. Reponen, S. Rothe, M. Safranova, C. Scheidenberger, A. Shindler, J. T. Singh, L. V. Skripnikov, A. V. Titov, S.-M. Udrescu, S. G. Wilkins, and X. Yang, Opportunities for fundamental physics research with radioactive molecules (2023), arXiv:2302.02165 [nucl-ex].
- [47] M. D. Barrett, B. DeMarco, T. Schaetz, V. Meyer, D. Leibfried, J. Britton, J. Chiaverini, W. M. Itano, B. Jelenković, J. D. Jost, C. Langer, T. Rosenband, and D. J. Wineland, Phys. Rev. A **68**, 042302 (2003).
- [48] T. R. Tan, J. P. Gaebler, Y. Lin, Y. Wan, R. Bowler, D. Leibfried, and D. J. Wineland, Nature **528**, 380 (2015).
- [49] D. Kielpinski, C. Monroe, and D. J. Wineland, Nature **417**, 709 (2002).
- [50] J. Keller, H. L. Partner, T. Burgermeister, and T. E. Mehlstäubler, Journal of Applied Physics **118**, 104501 (2015).
- [51] M. Borkowski, L. Reichsöllner, P. Thekkeppatt, V. Barbé, T. van Roon, K. van Druten, and F. Schreck, Active stabilization of kilogauss magnetic fields to the ppm level for magnetoassociation on ultranarrow feshbach resonances (2023), 2303.13682 [physics].
- [52] P. Yu and N. R. Hutzler, Phys. Rev. Lett. **126**, 023003 (2021).
- [53] L. Caldwell and M. R. Tarbutt, Phys. Rev. Res. **3**, 013291 (2021).
- [54] A. Jadbabaie, Y. Takahashi, N. H. Pilgram, C. J. Conn, Y. Zeng, C. Zhang, and N. R. Hutzler, Characterizing the fundamental bending vibration of a linear polyatomic molecule for symmetry violation searches (2023).
- [55] Y. Takahashi, C. Zhang, A. Jadbabaie, and N. R. Hutzler, Engineering field-insensitive molecular clock transitions for symmetry violation searches (2023).
- [56] G. Higgins, S. Salim, C. Zhang, H. Parke, F. Pokorny, and M. Henrich, New Journal of Physics **23**, 123028 (2021).
- [57] D. P. Nadlinger, P. Drmota, D. Main, B. C. Nichol, G. Araneda, R. Srinivas, L. J. Stephenson, C. J. Balance, and D. M. Lucas, Micromotion minimisation by synchronous detection of parametrically excited motion (2021), 2107.00056 [physics, physics:quant-ph].
- [58] L. Anderegg, B. L. Augenbraun, E. Chae, B. Hemmerling, N. R. Hutzler, A. Ravi, A. Collopy, J. Ye, W. Ketterle, and J. M. Doyle, Phys. Rev. Lett. **119**, 103201 (2017).
- [59] H. J. Briegel and R. Raussendorf, Phys. Rev. Lett. **86**, 910 (2001).
- [60] R. Verresen, N. Tantivasadakarn, and A. Vishwanath, Efficiently preparing Schrödinger's cat, fractons and non-abelian topological order in quantum devices (2022), 2112.03061 [cond-mat, physics:physics, physics:quant-ph].
- [61] J. Y. Lee, W. Ji, Z. Bi, and M. P. A. Fisher, Decoding measurement-prepared quantum phases and transitions: from ising model to gauge theory, and beyond (2022), 2208.11699 [cond-mat, physics:quant-ph].
- [62] T. V. Tscherbul, J. Ye, and A. M. Rey, Phys. Rev. Lett. **130**, 143002 (2023).
- [63] Y. Zhou, Y. Shagam, W. B. Cairncross, K. B. Ng, T. S. Roussy, T. Grogan, K. Boyce, A. Vigil, M. Pettine, T. Zelevinsky, J. Ye, and E. A. Cornell, Phys. Rev. Lett. **124**, 053201 (2020).
- [64] P. D. Gregory, L. M. Fernley, A. L. Tao, S. L. Bromley, J. Stepp, Z. Zhang, S. Kotochigova, K. R. A. Hazzard, and S. L. Cornish, arXiv:2306.02991 (2023).
- [65] C. Zhang, F. Pokorny, W. Li, G. Higgins, A. Pöschl, I. Lesanovsky, and M. Henrich, Nature **580**, 345 (2020).
- [66] A. Sunaga, M. Abe, M. Hada, and B. P. Das, Physical Review A **99**, 062506 (2019).
- [67] T. Fleig and D. DeMille, New Journal of Physics **23**, 113039 (2021).
- [68] M. Śmiałkowski and M. Tomza, Physical Review A **103**, 022802 (2021).
- [69] B. L. Augenbraun, J. M. Doyle, T. Zelevinsky, and I. Kozyryev, Phys. Rev. X **10**, 031022 (2020).
- [70] B. L. Augenbraun, Z. D. Lasner, A. Frenett, H. Sawaoka, A. T. Le, J. M. Doyle, and T. C. Steinle, Phys. Rev. A **103**, 022814 (2020).
- [71] J. J. Hudson, B. E. Sauer, M. R. Tarbutt, and E. A. Hinds, Phys. Rev. Lett. **89**, 023003 (2002).
- [72] J. Lim, J. R. Almond, M. R. Tarbutt, D. T. Nguyen, and T. C. Steinle, J. Mol. Spectrosc. **338**, 81 (2017).
- [73] P. Aggarwal, H. L. Bethlehem, A. Borschovsky, M. Denis, K. Esajas, P. A. B. Haase, Y. Hao, S. Hoekstra, K. Jungmann, T. B. Meijknecht, M. C. Mooij, R. G. E. Timmermans, W. Ubachs, L. Willmann, and A. Zapara, Eur. Phys. J. D **72**, 197 (2018).
- [74] T. C. Steinle, S. Frey, A. Le, D. DeMille, D. A. Rahmlow, and C. Linton, Physical Review A **84**, 012508 (2011).
- [75] R. F. G. Ruiz, R. Berger, J. Billowes, C. L. Binnery, M. L. Bissell, A. A. Breier, A. J. Brinson, K. Chrysaliidis, T. E. Cocolios, B. S. Cooper, K. T. Flanagan, T. F. Giesen, R. P. de Groote, S. Franchoo, F. P. Gustafsson, T. A. Isaev, A. Koszorus, G. Neyens, H. A. Perrett, C. M. Ricketts, S. Rothe, L. Schweikhard, A. R. Vernon, K. D. A. Wendt, F. Wienholtz, S. G. Wilkins, and X. F. Yang, Nature **581**, 396 (2020).
- [76] S.-M. Udrescu, S. Wilkins, A. Breier, R. F. G. Ruiz, M. Athanasakis-Kaklamanakis, M. Au, I. Belošević, R. Berger, M. Bissell, K. Chrysaliidis, T. Cocolios, R. Groote, A. Dorne, K. Flanagan, S. Franchoo, K. Gaul, S. Geldhof, T. Giesen, D. Hanstorp, R. Heinke, A. Koszorus, S. Kujanpää, L. Lalanne, G. Neyens, M. Nichols, H. Perrett, J. Reilly, S. Rothe, B. V. D. Borne, Q. Wang, J. Wessolek, X. Yang, and C. Zülch, Precision spectroscopy and laser cooling scheme of a radium-containing molecule (2023).
- [77] N. E. Shafer-Ray, Physical Review A **73**, 034102 (2006), publisher: American Physical Society.
- [78] R. J. Mawhorter, B. S. Murphy, A. L. Baum, T. J. Sears, T. Yang, P. M. Rupasinghe, C. P. McRaven, N. E. Shafer-Ray, L. D. Alphei, and J.-U. Grabow, Physical Review A **84**, 022508 (2011).

- [79] C. Zhu, H. Wang, B. Chen, Y. Chen, T. Yang, J. Yin, and J. Liu, *The Journal of Chemical Physics* **157**, 084307 (2022).